articles

molecular pharmaceutics

Iron Oxide Nanoparticles for Sustained Delivery of Anticancer Agents

Tapan K. Jain,[†] Marco A. Morales,[‡] Sanjeeb K. Sahoo,[†] Diandra L. Leslie-Pelecky,[‡] and Vinod Labhasetwar*[,†,§]

Department of Pharmaceutical Sciences, College of Pharmacy, Nebraska Medical Center, Omaha, Nebraska 68198-6025, Department of Physics & Astronomy and Center for Materials Research & Analysis, University of Nebraska—Lincoln, Lincoln, Nebraska 68588-0111, and Department of Biochemistry and Molecular Biology, University of Nebraska Medical Center, Omaha, Nebraska 68198-4525

Received January 18, 2005

Abstract: We have developed a novel water-dispersible oleic acid (OA)-Pluronic-coated iron oxide magnetic nanoparticle formulation that can be loaded easily with high doses of water-insoluble anticancer agents. Drug partitions into the OA shell surrounding iron oxide nanoparticles, and the Pluronic that anchors at the OA−water interface confers aqueous dispersity to the formulation. Neither the formulation components nor the drug loading affected the magnetic properties of the core iron oxide nanoparticles. Sustained release of the incorporated drug is observed over 2 weeks under in vitro conditions. The nanoparticles further demonstrated sustained intracellular drug retention relative to drug in solution and a dose-dependent antiproliferative effect in breast and prostate cancer cell lines. This nanoparticle formulation can be used as a universal drug carrier system for systemic administration of water-insoluble drugs while simultaneously allowing magnetic targeting and/or imaging.

Keywords: Sustained release; water-insoluble drugs; cellular uptake; breast cancer; targeting; tumor therapy; magnetic nanoparticles

Introduction

Magnetic nanoparticles offer exciting new opportunities toward developing effective drug delivery systems, as it is feasible to produce, characterize, and specifically tailor their functional properties for drug delivery applications.[1−6] An external localized magnetic field gradient may be applied to a chosen site to attract drug-loaded magnetic nanoparticles from blood circulation.[7] Drug targeting to tumors, as in other pathological conditions as well, is desirable since anticancer agents demonstrate nonspecific toxicities that significantly limit their therapeutic potentials.

* Author for correspondence. Mailing address: 986025 Nebraska Medical Center, Omaha, NE 68198-6025. Tel: (402) 559-9021. Fax: (402) 559-9543. E-mail: vlabhase@unmc.edu.

[†] Department of Pharmaceutical Sciences, College of Pharmacy, Nebraska Medical Center.

[‡] Department of Physics & Astronomy and Center for Materials Research & Analysis, University of Nebraska—Lincoln.

[§] Department of Biochemistry and Molecular Biology, University of Nebraska Medical Center.

(1) Gupta, A. K.; Berry, C.; Gupta, M.; Curtis, A. Receptor-mediated targeting of magnetic nanoparticles using insulin as a surface ligand to prevent endocytosis. *IEEE Trans. Nanobiosci.* **2003**, *2*, 255−261.

(2) Gupta, A. K.; Wells, S. Surface-modified superparamagnetic nanoparticles for drug delivery: preparation, characterization, and cytotoxicity studies. *IEEE Trans. Nanobiosci.* **2004**, *3*, 66−73.

(3) Zhang, Y.; Kohler, N.; Zhang, M. Surface modification of superparamagnetic magnetite nanoparticles and their intracellular uptake. *Biomaterials* **2002**, *23*, 1553−1561.

(4) Berry, C. C.; Charles, S.; Wells, S.; Dalby, M. J.; Curtis, A. S. The influence of transferrin stabilised magnetic nanoparticles on human dermal fibroblasts in culture. *Int. J. Pharm.* **2004**, *269*, 211−225.

(5) Tiefenauer, L. X.; Kuhne, G.; Andres, R. Y. Antibody-magnetite nanoparticles: in vitro characterization of a potential tumor-specific contrast agent for magnetic resonance imaging. *Bioconjugate Chem.* **1993**, *4*, 347−352.

(6) Alexiou, C.; Arnold, W.; Klein, R. J.; Parak, F. G.; Hulin, P.; Bergemann, C.; Erhardt, W.; Wagenpfeil, S.; Lubbe, A. S. Locoregional cancer treatment with magnetic drug targeting. *Cancer Res.* **2000**, *60*, 6641−6648.

10.1021/mp0500014 CCC: $30.25
Published on Web 04/21/2005

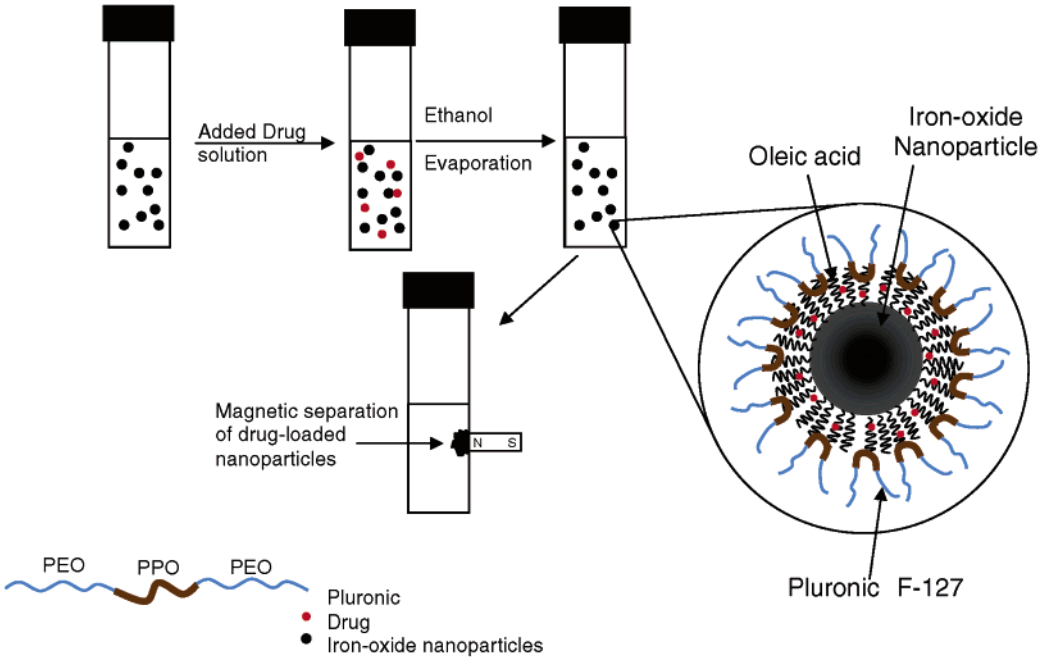

Figure 1. Schematic representing formulation of iron oxide nanoparticles and the process for drug loading.

The use of magnetic nanoparticles for drug delivery vehicles must address issues such as drug-loading capacity, desired release profile, aqueous dispersion stability, biocompatibility with cells and tissue, and retention of magnetic properties after modification with polymers or chemical reaction. Magnetic nanoparticles generally are coated with hydrophilic polymers such as starch or dextran (to impart aqueous dispersity to particles), and the therapeutic agent of interest is either chemically conjugated or ionically bound to the outer layer of polymer.[6,8−11] This approach is complex, involves multiple steps, and usually results in limited drug-loading capacity, and the bound drug dissociates within hours.[6] Rapid dissociation of drug from the carrier system may be less effective, especially in tumor therapy where chronic drug retention in the target tissue is required for therapeutic efficacy. Entrapping magnetic nanoparticles into other sustained-release polymeric drug carrier systems such as in microparticles formulated from poly-DL-lactide-*co*-glycolide (PLGA) or polylactides (PLL)[12] or in dendrimers and other polymers results in significant loss in magnetization (~40−50%) of the core magnetic material.[13,14] This decrease in magnetization negatively influences the magnetic targeting ability of the carrier system in vivo. The above approach is further limited by the amount of magnetic nanoparticles that can be incorporated into other drug delivery systems; for example, only 6 wt % α-Fe can be incorporated in silica nanospheres, which may not impart sufficient magnetic property to the formulation for effective targeting.[15]

We have developed a novel oleic acid (OA)-Pluronic-stabilized iron oxide magnetic nanoparticle formulation, and characterized it as a drug carrier system for anticancer agents. We hypothesized that hydrophobic drugs would partition into the OA shell surrounding the iron oxide nanoparticles, and Pluronic would anchor at the interface of the OA shell to confer an aqueous dispersity to the formulation (Figure 1). Our studies demonstrated that this approach formed a water-dispersible nanoparticle formulation, without the loss of mag-

(7) Alexiou, C.; Schmidt, A.; Klein, R.; Hulin, P.; Bergemann, C.; Arnold, W. Magnetic drug targeting: biodistribution and dependency on magnetic field strength. *J. Magn. Magn. Mater.* **2002**, *252*, 363−366.
(8) Mehta, R. V.; Upadhyay, R. V.; Charles, S. W.; Ramchand, C. N. Direct binding of protein to magnetic particles. *Biotechnol. Tech.* **1997**, *11*, 493−496.
(9) Koneracka, M.; Kopcansky, P.; Antalik, M.; Timko, M.; Ramchand, C. N.; Lobo, D.; Mehta, R. V.; Upadhyay, R. V. Immobilization of proteins and enzymes to fine magnetic particles. *J. Magn. Magn. Mater.* **1999**, *201*, 427−430.
(10) Koneracka, M.; Kopcansky, P.; Timko, M.; Ramchand, C. N.; de Sequeira, A.; Trevan, M. Direct binding procedure of proteins and enzymes to fine magnetic particles. *J. Mol. Catal. B: Enzym.* **2002**, *18*, 13−18.
(11) Bergemann, C.; Muller-Schulte, D.; Oster, J.; a Brassard, L.; Lubbe, A. S. Magnetic ion-exchange nano- and microparticles for medical, biochemical and molecular biological applications. *J. Magn. Magn. Mater.* **1999**, *194*, 45−52.
(12) Chattopadhyay, P.; Gupta, R. B. Supercritical CO_2 based production of magnetically responsive micro- and nanoparticles for drug targeting. *Ind. Eng. Chem. Res.* **2002**, *41*, 6049−6058.
(13) Strable, E.; Bulte, J. W. M.; Moskowitz, B.; Vivekanandan, K.; Allen, M.; Douglas, T. Synthesis and characterization of soluble iron oxide-dendrimer composites. *Chem. Mater.* **2001**, *13*, 2201−2209.
(14) Ramirez, L. P.; Landfester, K. Magnetic polystyrene nanoparticles with a high magnetite content obtained by miniemulsion processes. *Macromol. Chem. Phys.* **2003**, *204*, 22−31.
(15) Tartaj, P.; Serna, C. J. Synthesis of monodisperse superparamagnetic Fe/silica nanospherical composites. *J. Am. Chem. Soc.* **2003**, *125*, 15754−15755.

netic properties of the core iron oxide nanoparticles, and easy to load with high doses of water-insoluble anticancer agents.

Materials and Methods

Materials. Iron(III) chloride hexahydrate ($FeCl_3 \cdot 6H_2O$) pure granulated, 99%, iron(II) chloride tetrahydrate ($FeCl_2 \cdot 4H_2O$) 99+%, ammonium hydroxide (5 M), and oleic acid were purchased from Fisher Scientific (Pittsburgh, PA). Pluronic F-127 was received as a gift from BASF Corporation (Mt. Olive, NJ). Tween-80 was obtained from Sigma-Aldrich (St. Louis, MO). Doxorubicin hydrochloride was a generous gift from Dabur Research Foundation (Ghaziabad, India). Deionized water purged with nitrogen gas was used in all the steps involved in the synthesis and formulation of magnetic nanoparticles.

Synthesis of Magnetic Nanoparticles. Aqueous solutions of 0.1 M Fe(III) (30 mL) and 0.1 M Fe(II) (15 mL) were mixed, and 3 mL of 5 M ammonia solution was added dropwise over 1 min with stirring on a magnetic stir plate. The stirring continued for 20 min under a nitrogen-gas atmosphere. The particles obtained were washed 3 times using ultracentrifugation (30000 rpm for 20 min at 10 °C) with nitrogen purged water. The iron oxide nanoparticle yield, determined by weighing of the lyophilized sample of the preparation, was 344 mg.

Formulations of Magnetic Nanoparticles. Formulations of iron oxide nanoparticles were developed, first by optimizing the amount of OA required to coat iron oxide nanoparticles completely, and then by optimizing the amount of Pluronic required to form an aqueous dispersion of OA-coated nanoparticles. To study the effect of OA, formulations with different weight ratios of OA to iron oxide nanoparticles were prepared. For this purpose, OA was added (6−250 mg corresponding to 1.7 wt % to 41.0 wt % of the total formulation weight, i.e., iron oxide nanoparticles plus OA) to the above solution of Fe(III) and Fe(II) following the addition of ammonia solution. The formulations were heated to 80 °C while being stirred for 30 min to evaporate the ammonia, and then cooled to room temperature. The black precipitate thus obtained was washed twice with 15 mL of water; the excess OA formed an emulsion as apparent from the turbid nature of the supernatant. The precipitate was lyophilized for 2 days at −60 °C and 7 μmHg vacuum (LYPHLOCK 12 LABCONCO, Kansas City, MO).

To study the effect of Pluronic on aqueous dispersity of OA-coated iron oxide nanoparticles, different amounts of Pluronic (25−500 mg corresponding to 5.6 wt % to 54.0 wt % of total formulation weight, i.e., iron oxide nanoparticles plus OA plus Pluronic) were added to the optimized composition of OA-coated iron oxide nanoparticles as determined above. Pluronic was added to the dispersion of OA-coated nanoparticles (the dispersion was cooled to room temperature but not lyophilized) and stirred overnight in a closed container to minimize exposure to atmospheric oxygen to prevent oxidation of the iron oxide nanoparticles. These particles were washed with water to remove soluble salts and excess Pluronic. Particles were separated by ultracentrifugation at 30000 rpm (Optima LE-80K, Beckman, Palo Alta, CA) using a fixed angle rotor (50.2 Ti) for 30 min at 10 °C. The supernatant was discarded, and the sediment was redispersed in 15 mL of water by sonication in a water-bath sonicator (FS-30, Fisher Scientific) for 10 min. The suspension was centrifuged as above, and the sediment was washed three times with water. Nanoparticles were resuspended in water by sonication as above for 20 min and centrifuged at 1000 rpm for 20 min at 7−11 °C to remove any large aggregates. The supernatant containing OA-Pluronic-stabilized nanoparticles was collected and used for drug loading as described below.

Physical Characterization of Nanoparticles. Particle Size Determination Using Dynamic Laser Light Scattering and ζ Potential Measurements. For measuring the particle size of OA-coated nanoparticles, each sample was dispersed in hexane (0.1 mg/mL) using a water-bath sonicator for 5 min and the particle size was measured using a glass cuvette (ZetaPlus ζ potential analyzer, Brookhaven Instruments Corporation, Holtsville, NY). An identical procedure was used for measuring the particle size of OA-Pluronic stabilized nanoparticles, except that the nanoparticle suspension was prepared in water (2 μg/mL) and the size was measured using a polystyrene cuvette (Brookhaven Instruments Corporation). The same suspension was used for measuring the ζ potential of particles (Brookhaven Instruments Corporation).

Transmission Electron Microscopy (TEM). A drop of an aqueous dispersion of OA-Pluronic-stabilized nanoparticles was placed on a Formvar-coated copper TEM grid (150 mesh, Ted Pella Inc. Redding, CA) and was allowed to air-dry. Particles were imaged using a Philips 201 transmission electron microscope (Philips/FEI Inc., Briarcliff, Manor, NY). The NIH ImageJ software was used to calculate the mean particle diameter from the TEM photomicrograph. Diameters of 50 particles were measured to calculate the mean particle diameter.

X-ray Diffraction (XRD). The XRD analysis of lyophilized samples of OA-coated iron oxide nanoparticles was carried out using a Rigaku D-Max/B horizontal diffractometer with Bragg−Brentano parafocusing geometry (Rigaku, The Woodlands, TX). The equipment uses a Copper target X-ray tube with Cu Kα radiation. The parameters chosen for the measurement were 2θ steps of 0.02°, 6 s of counting time per step, and 2θ range from 20° to 80°. Approximately 15 mg of lyophilized sample was sprinkled onto a low-background quartz XRD holder coated with a thin layer of silicone grease to retain the sample.

Thermogravimetric Analysis (TGA). Lyophilized samples (~2 mg) of nanoparticles (OA-coated and OA-Pluronic-coated) were placed in aluminum sample cells (Fisher Scientific), and a thermogram for each sample was obtained using a Shimadzu thermogravimetric analyzer (TGA50, Shimadzu Scientific Instruments Inc., Columbia, MD). Samples were heated at the rate of 15 °C/min under the flow of nitrogen gas set at an outlet pressure of 6−10 kg/cm^2.

Fourier Transform Infrared (FT-IR) Spectroscopy. Measurements were carried out on a Nicolet Avatar 360 FT-

IR spectrometer (Thermo Nicolet Corp.), and each spectrum was obtained by averaging 32 interferograms with resolution of 2 cm^{-1}. Pellets for FT-IR analysis were prepared by mixing the lyophilized samples of iron oxide nanoparticle formulations with spectroscopic grade KBr powder.

Magnetization Studies. Magnetic measurements were carried out using a Quantum Design MPMS SQUID magnetometer, and room temperature measurements were performed using a MicroMag 2900 alternating gradient field magnetometer (AGFM, Princeton Measurements Corp). Zero-field-cooled (ZFC) and field-cooled (FC) magnetization measurements as functions of temperature were performed. For the ZFC measurement, each sample was cooled from 300 to 10 K in zero field and the magnetization was measured as a function of temperature at 100 Oe as the sample was warmed. For the FC measurement, the sample was cooled in the measuring field and the magnetization was measured as the sample was cooled. Magnetization measurements as a function of field $M(H)$ were performed at 10 and 300 K. At 10 K, the saturation magnetization M_S and the coercive field H_C were determined by fitting the magnetization curve with an analytical ferromagnetic model and a diamagnetic contribution (χ) due to the background.[16,17]

$$M(H) = \frac{2}{\pi} M_S \arctan\left(\left(\frac{H}{H_C} \pm 1\right) \tan\left(\frac{\pi s}{2}\right)\right) + \chi H$$

At 300 K, the $M(H)$ loops were fit to a Langevin function weighted by a log-normal distribution of particle sizes.

Drug Loading in Magnetic Nanoparticles. Doxorubicin was used as a model anticancer agent. For incorporation in nanoparticles, the hydrochloride salt of the drug (DOX·HCl) was converted to water-insoluble base (DOX) using a procedure described previously.[18] A methanolic solution of DOX (600 μL, 5 mg/mL) was added dropwise with stirring to an aqueous dispersion of OA-Pluronic-stabilized iron oxide nanoparticles (30 mg of particles in 7 mL of water) (Figure 1). Stirring was continued overnight (~16 h) to allow partitioning of the drug into the OA shell surrounding iron oxide nanoparticles. Drug-loaded nanoparticles were separated from the unentrapped drug using a magnet (12200 G, Edmund Scientific, Tonawanda, NY). Nanoparticles were washed twice by being resuspended in distilled water and separated as above using the magnetic field.

To determine drug loading, a 200 μL aliquot of nanoparticle suspension was lyophilized and the weight of the lyophilized sample was measured. For drug extraction, 2 mL of 12.5% v/v methanolic solution in chloroform was added to the dried sample. The samples were shaken for 24 h (Environ shaker, model no. 3527, Lab-Line instruments, Melrose Park, IL). Since DOX has greater solubility in this combination of solvents than in methanol or chloroform alone, it was used for the extraction. Nanoparticles were centrifuged for 10 min at 16000*g* using an Eppendorf microcentrifuge (5417R, Eppendorf-Netheler-Hinz-GmbH, Hamburg, Germany). An aliquot (100 μL) of the supernatant was diluted to 1 mL with a methanol−chloroform mixture, and the drug concentration was determined using a fluorescence spectrophotometer (Varian, Cary Eclipse, Walnut Creek, CA) at λ_{ex} = 485 nm and λ_{em} = 591 nm. A standard plot was prepared under identical conditions to calculate the amount of drug loaded in the nanoparticles. There was no further increase in the amount of drug extracted when nanoparticles were kept for extraction for more than 24 h.

Kinetics of DOX Release from Magnetic Nanoparticle. DOX-loaded nanoparticles were suspended in PBS buffer (154 mM, pH = 7.4 PBS containing 0.1% w/v Tween-80, PBS-Tween-80). The release study was carried out in double diffusion cells, with the donor chamber filled with 2.5 mL of nanoparticle suspension (2 mg/mL) and the receiver chamber with 2.5 mL PBS-Tween-80. The chambers were separated by a PVDF membrane of 0.1 μm porosity (Durapore Millipore, VVLP, Billerica, MA). Nanoparticles do not cross the membrane, but drug can diffuse freely. This was confirmed by analyzing the receiver chamber samples for iron content using atomic absorption spectroscopy (Varian 220FS flame atomic absorption spectrophotometer, Walnut Creek, CA). Cells were left on a shaker rotating at 110 rpm at 37 °C (Environ shaker), and buffer from the receiver chambers was completely withdrawn at different time intervals and replaced with fresh buffer. Tween-80 was used in the buffer to maintain sink conditions during the release study. The samples were lyophilized and extracted with 12.5 vol % methanol in chloroform. DOX levels in the extracted samples were analyzed by measuring the fluorescence intensity at λ_{ex} = 485 nm and λ_{em} = 591 nm. A standard plot for DOX was prepared under identical conditions, i.e., dissolving drug in Tween-80 solution, lyophilizing the samples, and extracting the drug as described above.

Cell Culture. PC3 (prostate cancer) and MCF-7 (breast cancer) cells purchased from American Type Culture Collection (ATCC, Manassas, VA) were grown in RPMI 1640 medium supplemented with 10% fetal bovine serum and 100 μg/mL penicillin G and 100 μg/mL streptomycin (Gibco BRL, Grand Island, NY) at 37 °C in a humidified and 5% CO_2 atmosphere.

Mitogenic Assay. PC3/MCF-7 cells were seeded at 3000 per well in 96-well plates (MICROTEST Becton Dickinson Labware, Franklin Lakes, NJ) 24 h prior to the experiment. Different concentrations of DOX (0.1 μM to 100 μM), either loaded in nanoparticles or as solutions, were added. For studies with DOX as a solution, a stock solution of hydrochloride salt (590 μg/mL) in 77% ethanol was prepared and 50 μL of this solution was diluted to 9 mL with medium containing serum to prepare a drug solution of 100 μM

(16) Stearns, M. B.; Cheng, Y. Determination of para- and ferromagnetic components of magnetization and magnetoresistance of granular Co/Ag films. *J. Appl. Phys.* **1994**, *75*, 6894−6899.

(17) Noyau, R. H.; Middleton, B. K.; Miles, J. J.; Mackintosh, N. D. Modeliing digital recording in thin film media. *IEEE Trans. Magn.* **1988**, *24*, 2494−2496.

(18) Yolles, S.; Aslund, B.; Morton, J. F.; Olson, O. T.; Rosenberg, B. Timed-released depot for anticancer agents. II. *Acta Pharm. Suec.* **1978**, *15*, 382−388.

concentration. The maximum amount of alcohol used did not exceed 0.4 vol %, which does not affect cell growth. Drug solutions of lower concentrations were prepared by appropriate dilution of the above drug solution with serum-containing medium. A stock dispersion of drug-loaded iron oxide nanoparticles was prepared in serum-containing medium so that the drug concentration was 100 μM. Nanoparticles without drug and medium were used as controls. Medium in the wells was replaced either with drug in solution or with a dispersion of drug-loaded nanoparticles as described above. The medium was changed at 2 and 4 days following drug treatment, but no further dose of the drug was added. Cell viability was determined at 5 days posttreatment using a standard MTS assay (CellTiter 96 AQ_{ueous}, Promega, Madison, WI). To each well was added 20 mL of reagent, the plates were incubated for 75 min at 37 °C in the cell culture incubator, and color intensity was measured at 490 nm using a plate reader (BT 2000 Microkinetics Reader, BioTek Instruments, Inc., Winooski, VT). The effect of drug on cell proliferation was calculated as the percentage inhibition in cell growth with respect to the respective controls.

Confocal Laser Scanning Microscopy for Cellular Uptake of Drug. MCF-7 cells were seeded in Bioptechs plates (Bioptechs, Butler, PA) at 50000 cells/plate in 1 mL of serum-containing medium 24 h prior to the experiment. A dispersion of drug-loaded or void nanoparticles and drug solution (10 μM) was prepared in cell-culture medium as described above. Cells were incubated either with drug in solution or a with a dispersion of drug-loaded nanoparticles for 2 h, 24 h, and 48 h. Cells were washed three times with PBS before being imaged under a confocal microscope (Zeiss Confocal microscope LSM410 equipped with an argon−krypton laser, Thornwood, NY) at $\lambda_{ex} = 488$ nm and a long-pass filter with a cut-on filter of 515 nm for detecting the emission light.

Statistical Analysis. Statistical analyses were performed using a Student's *t* test. The differences were considered significant for p values of <0.05.

Results

The hydrophilic nature of the iron oxide nanoparticle surface precludes their dispersal in nonpolar solvents such as hexane and chloroform. OA is chemisorbed on the surface of the nanoparticles, which makes the particles hydrophobic; thus they become dispersible in nonpolar solvents. Dispersity of OA-coated iron oxide nanoparticles in an organic solvent thus was used to determine the concentration of OA required for complete coating of nanoparticle surface. Complete coverage of iron oxide nanoparticles with OA is critical to achieving uniform anchoring of Pluronic onto these particles for their eventual dispersion in water. Increasing OA concentration reduced particle sedimentation in hexane (Figure 2a) as well as the mean particle size and polydispersity index (Figure 2b). The above data indicated that ~23 wt % (of the total formulation content) or more OA is required to disperse iron oxide nanoparticles in hexane (Figure 2b). To determine the amount of OA that can be associated to the iron oxide nanoparticles, the formulations with different concentration of OA were characterized for mass loss using TGA. The mass loss data demonstrated an increase in bound OA to iron oxide nanoparticles with an increase in OA concentration (Figure 2c); however, no significant difference in the mass loss was observed when 17 or 23 wt % OA was used, suggesting a saturation binding of OA to particle surface around these concentrations. The TGA data demonstrated that ~18 wt % OA remains bound to nanoparticles when 23 wt % OA was used in the formulation, i.e., 75 wt % of the added OA was bound to the iron oxide nanoparticles and could not be washed off. The particle-size-analysis data in hexane demonstrated that a higher amount of OA (30 wt %) was required for dispersion of iron oxide nanoparticles; however, the TGA demonstrated that ~18 wt % OA can be bound to nanoparticles. This discrepancy in the amount of OA required could be due to partial desorption of OA from the nanoparticle surface when they were dispersed in hexane.

TGA and FT-IR spectroscopy of OA-coated iron oxide nanoparticles indicated chemisorption of OA at the iron oxide nanoparticle surface and its multilayer deposition at higher than 17 wt % OA concentration. The TGA data demonstrated that the mass loss in OA-coated nanoparticles occurs at about 300 °C (range 210−400 °C), which is higher than that for the pure OA (250 °C, range 150−400 °C) (Figure 2d). This shift in the temperature could be due to chemisorption of OA on the iron oxide nanoparticle surface, requiring higher temperature for the vaporization of bound OA. The peak at 1705 cm^{-1} in the FT-IR spectra of pure OA is due to the C═O stretch dimer H-bonded, the broad peak at around 3000 cm^{-1} is due to the O−H stretch dimer H-bonded, and the peaks at 2853 cm^{-1} and 2922 cm^{-1} correspond to the symmetric and asymmetric CH_2 stretching modes, respectively (Figure 3a). The spectra of OA-coated iron oxide nanoparticles, however, indicate the absence of the C═O stretch at 1705 cm^{-1}, suggesting binding of the carboxylic group of OA to the iron oxide nanoparticles (Figure 3b). The spectra of pure iron oxide (Figure 3bA) and OA-coated iron oxide nanoparticles (Figure 3bE) show that both stretching modes appear in the spectrum: the symmetric stretching band is located at 1435 cm^{-1} and the asymmetric band ranges from 1530 cm^{-1} to 1570 cm^{-1}. The additional feature that appears at 1712 cm^{-1} could be due to the C═O stretch monomer. This peak starts to appear for concentrations of OA higher than 17 wt % (Figure 3c) and could be evidence of OA bilayer formation. A strong and broad peak at 3454 cm^{-1} suggests chemisorption of OA onto iron oxide nanoparticles; however, the intensity of this peak decreased with increasing OA concentration. The suppression of the OH vibrational mode in the 3000−3700 cm^{-1} region has been related to evidence of host−guest interaction as a consequence of water release upon chemisorption of OA. Figure 3d shows the ratio of the intensities of the CH_2 symmetric stretch mode to the OH stretch mode versus the relative concentration of OA to iron oxide. The curve reaches a nearly constant value when the OA concentration is about 17 wt %, indicating that OA has reacted with most of the

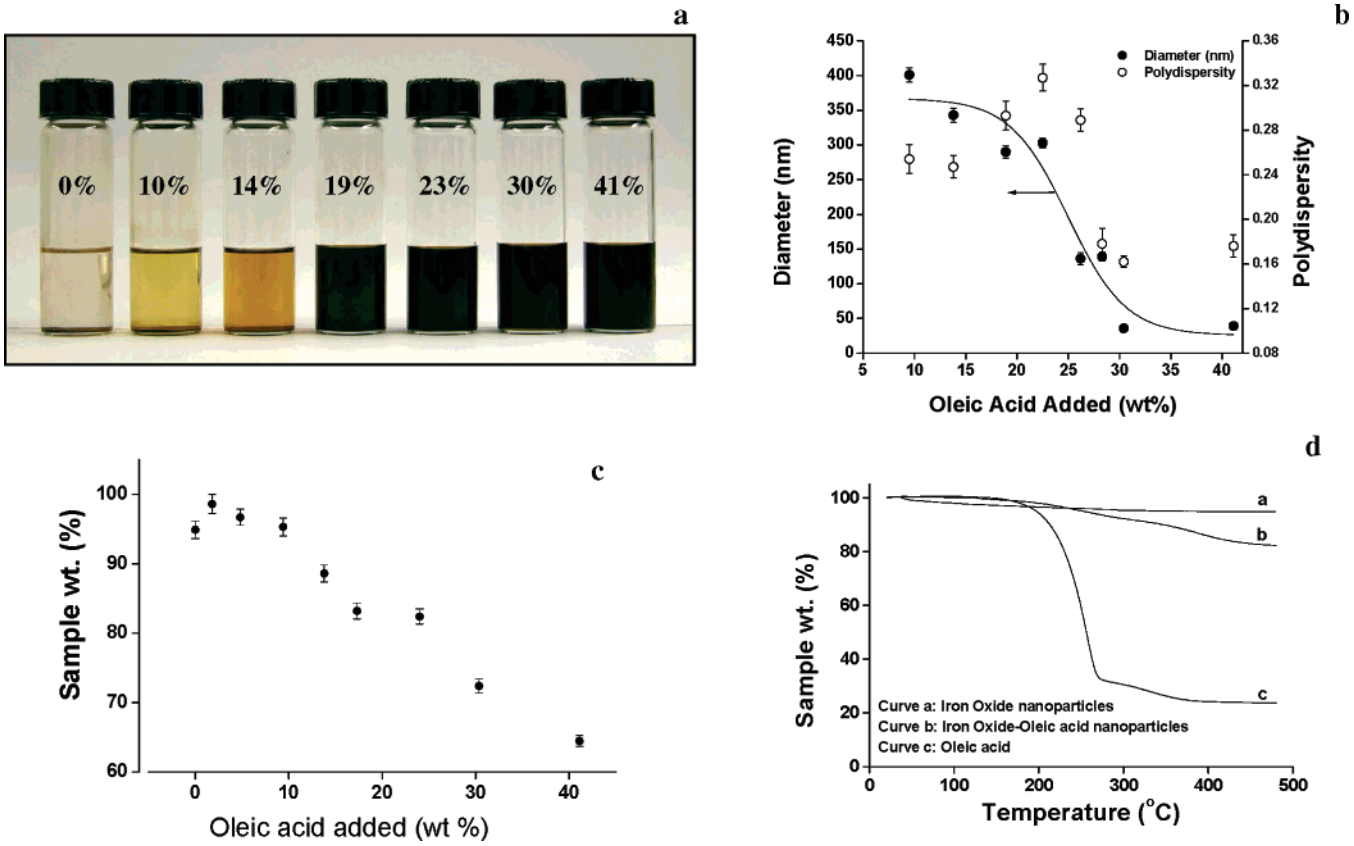

Figure 2. Effect of OA concentration on (a) sedimentation of iron oxide nanoparticles in hexane after 2 days; (b) mean particle size and polydispersity index of OA-coated iron oxide nanoparticles in hexane (data as mean ± SEM, $n = 10$, a nonlinear square fitting was used to connect data points); (c) mass loss by thermogravimetric analysis of different formulations of OA-coated iron oxide nanoparticles (data as mean ± SEM, $n = 3$; and (d) typical thermograms of iron oxide nanoparticles, OA, and OA-coated iron oxide nanoparticles (a representative from three different runs).

active binding sites on the iron oxide nanoparticle surfaces. Using the average particle diameter of 9.3 nm for iron oxide nanoparticles, at 17 wt % OA concentration, the surface area occupied per OA molecule was estimated to be 0.34 nm^2; whereas, at 30 wt % OA concentration, it was 0.21 nm^2. This decrease in surface area per OA molecule at higher concentration of OA suggests the formation of a multilayer coating. The TGA analysis of OA-coated iron oxide nanoparticles also demonstrated multilayer deposition of OA at higher concentrations (Figure 2c). On the basis of these observations, the formulation containing 23 wt % OA with respect to total formulation weight, which is slightly in excess of that required for monolayer adsorption of OA, was used for further studies.

The objective of the following set of experiments was to determine the amount of Pluronic required to disperse OA-coated iron oxide nanoparticles in water. Increasing the Pluronic concentration up to 100 mg (19 wt % with respect to total formulation weight) reduced the particle size, but further increase in Pluronic concentration had an insignificant effect on particle size when measured by dynamic laser light scattering technique (Figure 4a). The mass loss from the TGA analysis indicates that 71 wt % of the added Pluronic was associated with nanoparticles when 100 mg of Pluronic was added in the formulation. That there was no change in the particle size with further increase in Pluronic could be because of saturation of the OA interface around nanoparticles with Pluronic, thus not further influencing the dispersion of particles in water. The mean particle size measured by dynamic laser light scattering analysis was 193 nm with a polydispersity index of 0.262 (Figure 4a), whereas the particle size calculated by analyzing the XRD peaks using the integral-breath method was 9.2 ± 0.8 nm and that from TEM was 11 ± 2 nm (Figure 4b). The larger particle size by laser light scattering, which measures the hydrodynamic diameter, could be due in part to the contribution of OA and Pluronic associated with nanoparticles and its hydration with water. The high polydispersity index also suggests that there is some aggregation of OA-Pluronic-stabilized nanoparticles when dispersed in water. This aggregation could be the result of incomplete dispersion of OA-coated nanoparticles in Pluronic or due to their flocculation because these nanoparticles have almost neutral ζ potential ($\zeta = -0.22$ mV). The ζ potential of uncoated iron oxide nanoparticles is −13.40 mV, which could have been masked by the bound OA and the coating of nonionic Pluronic. Since the concentration of Pluronic used in the formulation is below the critical micelle concentration[19] (cmc = 20 mg/mL), it is possible that Pluronic could have been anchored at the

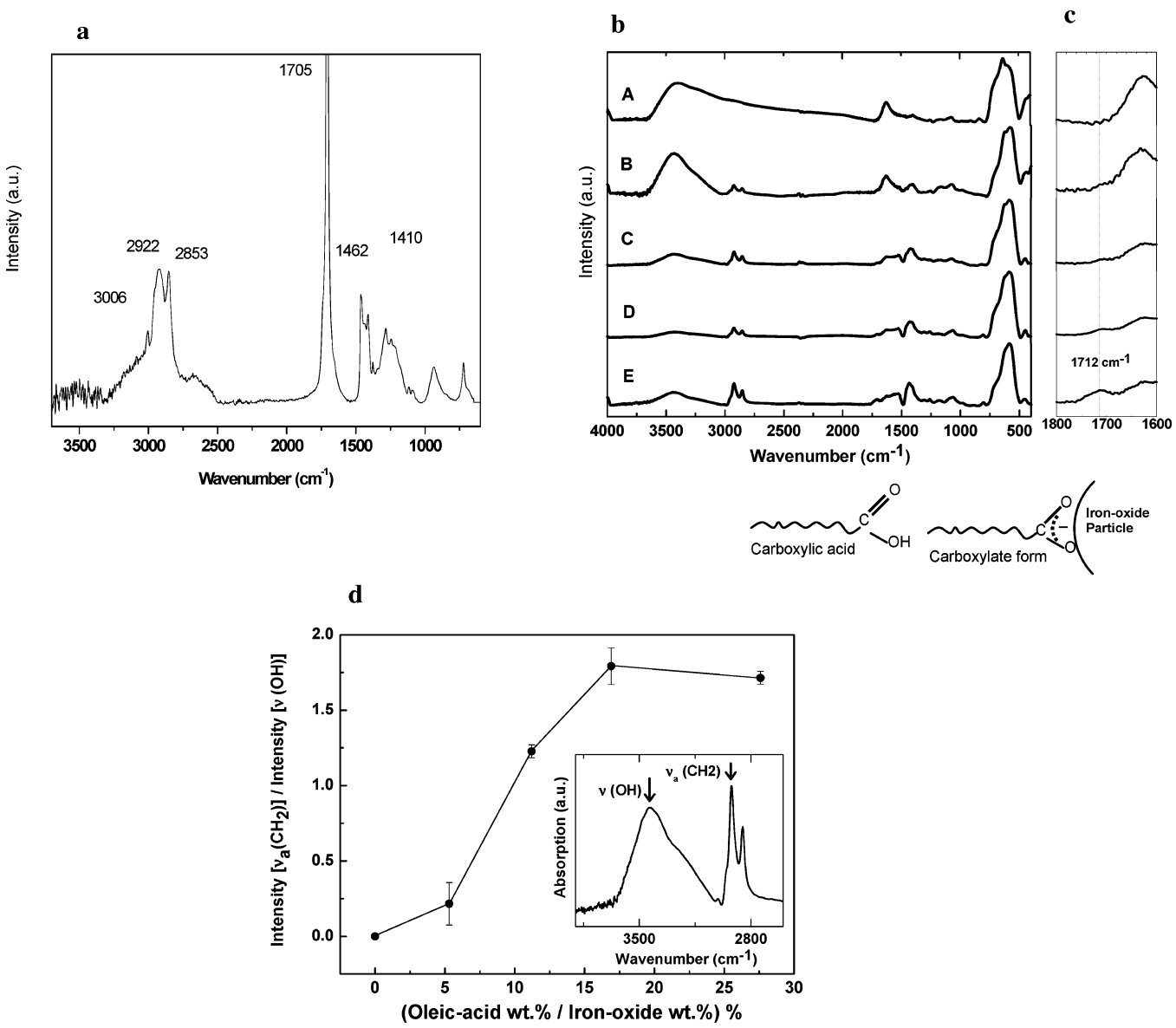

Figure 3. (a) FT-IR spectrum of pure OA. (b) FT-IR spectra of OA-coated iron oxide nanoparticles: (A) pure iron oxide; (B) 5 wt % OA relative to iron oxide; (C) 11 wt % OA relative to iron oxide; (D) 17 wt % OA relative to iron oxide; and (E) 23 wt % OA relative to iron oxide. (c) Zoom of the FT-IR spectra in the range of 1800−1600 cm^{-1}. (d) Relative intensities of the CH_2 symmetric stretch mode to the OH stretch mode versus the relative concentration of OA to the iron oxide (data as mean ± SEM from 32 spectral scans).

interface of OA-coated nanoparticles in the form of a multilayer deposit rather than as micelles.

The FT-IR spectra of OA-Pluronic-stabilized iron oxide nanoparticles at different concentrations of OA and Pluronic demonstrated that there is no bonding of Pluronic to the particle surface in the absence of OA. This is evident from the identical spectra of Pluronic iron oxide nanoparticles and pure iron oxide nanoparticles (Figure 4cA and 4cC); however, Pluronic bonding to nanoparticles increased with increasing OA concentration. The FT-IR spectra of OA-Pluronic-stabilized iron oxide nanoparticles demonstrated broad bands around 1250−1000 cm^{-1} that are due to the CH_2 rocking and C−O−C stretch vibrations of Pluronic. The FT-IR spectrum developed strong and well-defined bands at around 1113 cm^{-1}, typical of a block copolymer in the optimal formulation in which OA completely covers the iron oxide nanoparticle surface (Figure 4cE). The peaks at 2853 and 2920 cm^{-1} in the spectra are due to chemisorbed OA.

The composition of the iron oxide nanoparticle formulation as optimized above was 70.1 wt % iron oxide, 15.4 wt % OA, and 14.5 wt % Pluronic (nominal composition was 63.0 wt % iron oxide, 18.3 wt % OA, and 18.7 wt % Pluronic). The composition was determined on the basis of the mass-loss data from the TGA of OA-coated and OA-Pluronic

(19) Desai, P. R.; Jain, N. J.; Sharma, R. K.; Bahadur, P. Effect of additives on the micellization of PEO/PPO/PEO block copolymer F127 in aqueous solution. *Colloid Surf., A* **2001**, *178*, 57−69.

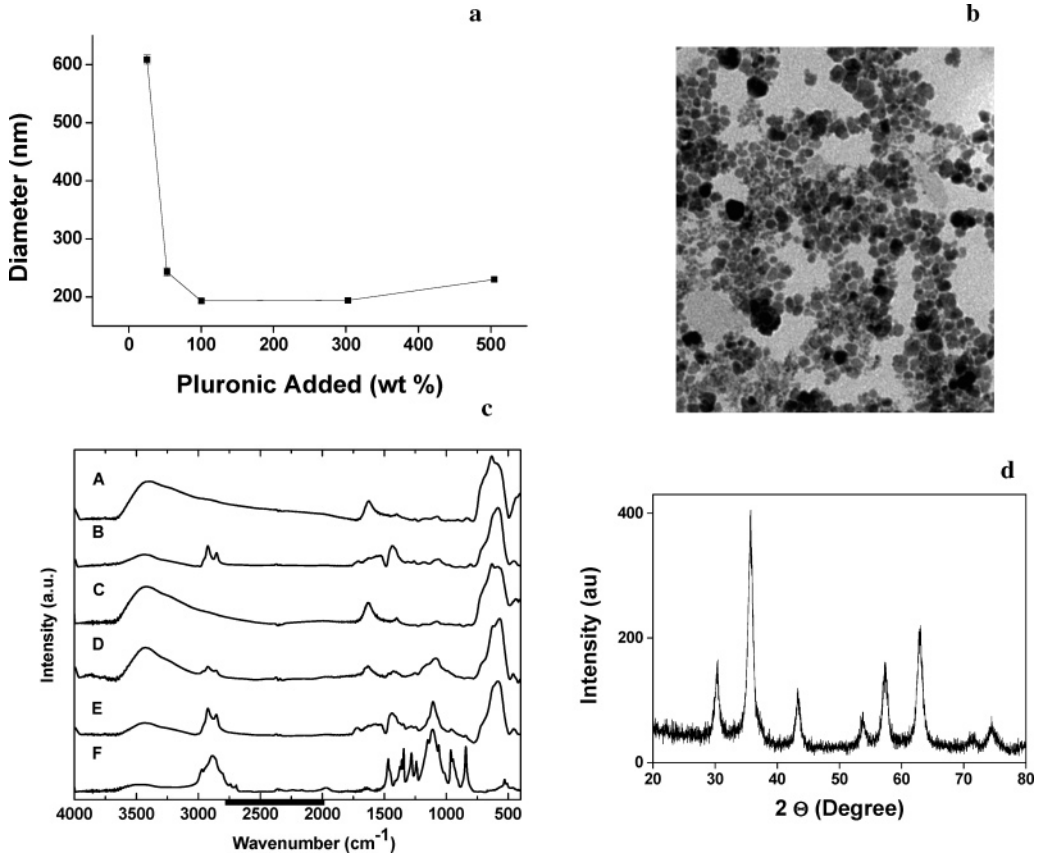

Figure 4. (a) Effect of different concentration of Pluronic on particle size of OA-coated iron oxide nanoparticles in water as measured by laser light scattering method (data as mean ± SEM, $n = 10$). (b) TEM of OA-Pluronic stabilized iron oxide nanoparticles. (c) FT-IR spectra: (A) pure iron oxide; (B) 78.4 wt % iron oxide, 21.6 wt % OA; (C) 40.4 wt % iron oxide, 0.0 wt % OA, 59.6 wt % Pluronic F127; (D) 54.8 wt % iron oxide, 2.7 wt % OA, 42.5 wt % Pluronic F127; (E) 70.1 wt % iron oxide, 15.4 wt % OA, 14.5 wt % Pluronic F127; and (F) pure Pluronic F127. (d) XRD powder pattern of OA-Pluronic stabilized iron oxide nanoparticles.

Table 1. Effect of OA and Pluronic on Magnetic Properties of Iron Oxide Nanoparticles at 10 K[a]

samples	saturation magnetization M_S (emu/g)	T_{max} (K)	coercive field H_C (Oe)
iron oxide nanoparticles	66.1 ± 0.1	215 ± 7	201 ± 11
OA-Pluronic-stabilized iron oxide nanoparticles	86.1 ± 0.5	170 ± 5	158 ± 05
drug-loaded OA-Pluronic-stabilized iron oxide nanoparticles	88.8 ± 0.5	160 ± 5	151 ± 06

[a] Saturation magnetization is normalized to the weight of magnetite.

stabilized formulations. The XRD spectra of OA-Pluronic-stabilized iron oxide nanoparticles exhibited peaks that correspond to both maghemite (Fe_2O_3) and magnetite (Fe_3O_4) (Figure 4d); however, the value of the magnetic moment as measured by SQUID and normalized to the amount of iron determined by AAS suggests that the majority of the iron oxide is magnetite.

The saturation magnetization M_S, the coercivity H_C, and the peak temperature of the ZFC magnetization of OA-Pluronic-stabilized iron oxide nanoparticles are shown in Table 1. The M_S values were normalized assuming 100% magnetite for simplicity using the iron mass as determined by atomic absorption spectroscopy.[20] Figure 5 shows typical hysteresis curves at 10 and 300 K for the optimized nanoparticle formulation. The hysteresis loops have negligible coercivity at room temperature, and the magnetization at 1.2 T (after subtraction of a diamagnetic background) was

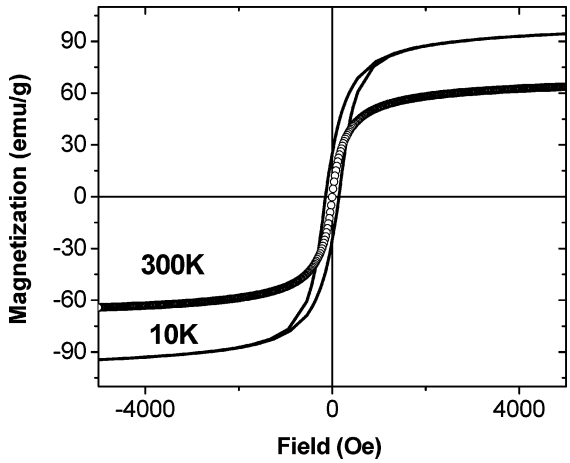

Figure 5. Magnetization as a function of field OA-Pluronic-stabilized iron oxide nanoparticles, measured at 10 K (solid line) and 300 K (circles).

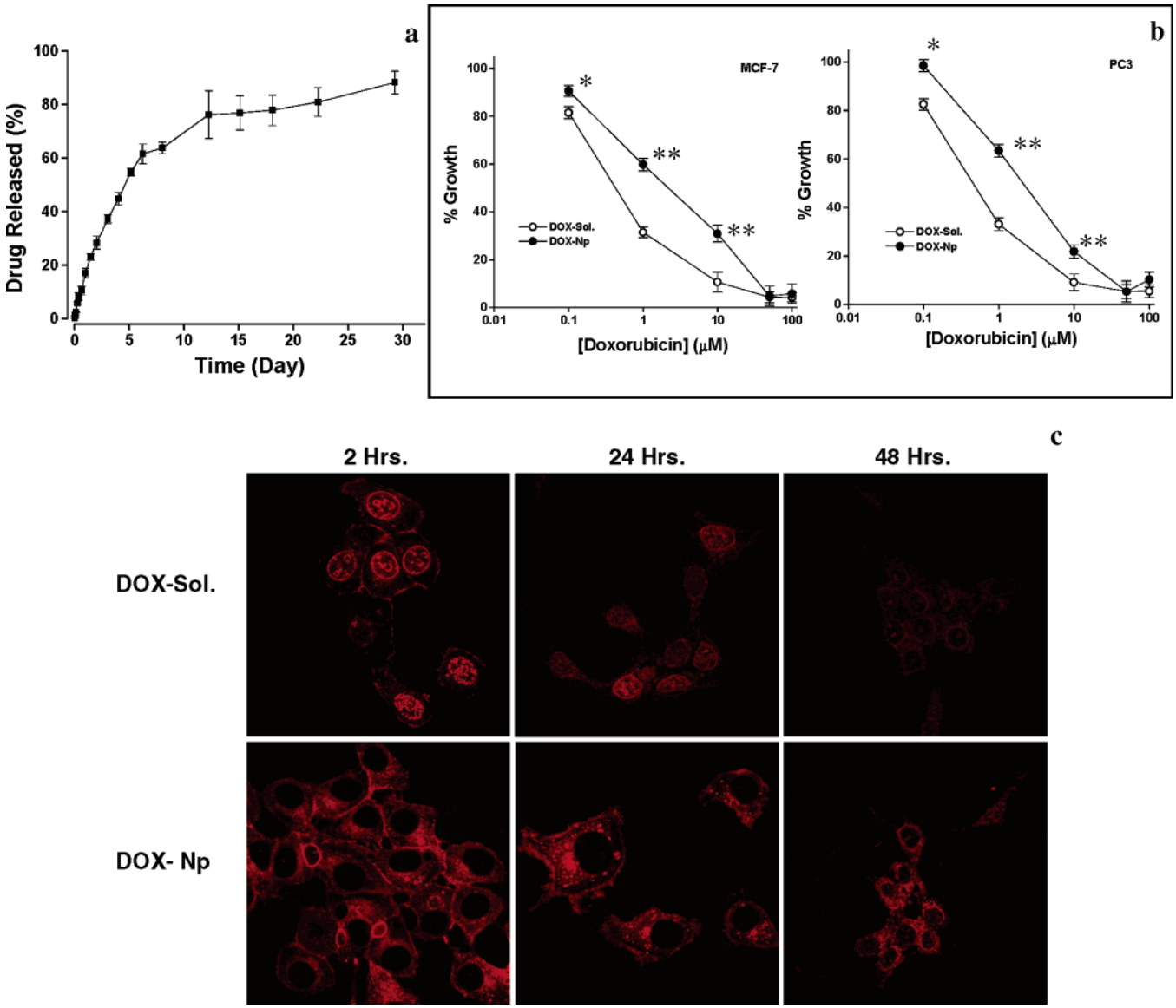

Figure 6. (a) Release of doxorubicin in vitro from drug-loaded OA-Pluronic-stabilized iron oxide nanoparticles. (b) Antiproliferative activity of drug-loaded nanoparticles and drug in solution in MCF-7 and PC3 cells. Data as mean ± SEM ($n = 6$). * = $p < 0.05$, ** = $p < 0.005$, *** = $p < 0.001$. p values calculated for DOX-Np vs DOX-Sol. (c) Confocal laser scanning microscopic images of MCF-7 cells incubated for 2, 24, and 48 h with drug-loaded nanoparticles or drug in solution. Original magnification, 100×.

59.2 ± 0.8 emu/$g_{magnetite}$ for OA-Pluronic-stabilized iron oxide nanoparticles and 45.1 ± 0.8 emu/$g_{magnetite}$ for uncoated iron oxide nanoparticles. The hysteresis loops measured at 300 K were fit to a Langevin function weighted by a log-normal distribution of particle sizes to determine the magnetic volume of the nanoparticle. The mean magnetic diameter was 9.9 nm ± 5.5 nm (means ± standard deviation). The nanoparticles were not superparamagnetic at 10 K. The saturation magnetization at 10 K for OA-Pluronic-stabilized iron oxide nanoparticles was higher than that of unmodified iron oxide nanoparticles, and hysteresis developed. Table 1 shows the ZFC peak position (T_{max}) for the uncoated iron oxide nanoparticles and for the optimized nanoparticle formulation. The peak temperature was determined from the derivative of the magnetization versus temperature.

DOX loading in formulation was 8.2 ± 0.5 wt % (i.e., 82 μg of drug/mg of nanoparticles) with an encapsulation efficiency of 82% (i.e., 82% of the added drug was entrapped in the formulation). Since a magnetic field was used to separate drug-loaded magnetic nanoparticles, any drug that did not partition in the OA shell surrounding the nanoparticles was retained in the aqueous phase. Drug loading did not change the magnetic properties of the formulation (Table 1). The release of DOX from nanoparticles was sustained, with about 28% cumulative drug release occurring in 2 days and about 62% over 1 week (Figure 6a).

Control nanoparticles without drug did not show a cytotoxic effect in the concentration range of 0.1−100 μg/mL,

(20) Pepic, I.; Jalsenjak, N.; Jalsenjak, I. Micellar solutions of triblock copolymer surfactants with pilocarpine. *Int. J. Pharm.* **2004**, *272*, 57−64.

as the cell growth rate with nanoparticles was the same as that of the medium control (data not shown). The data thus indicate that surface modification with OA and Pluronic does not cause a toxic effect. Drug-loaded nanoparticles, however, demonstrated a dose-dependent cytotoxic effect in both MCF-7 and PC3 cells, which was slightly lower than that observed with equivalent doses of the drug in solution (Figures 6b). This could be because of the sustained drug-release property of the nanoparticles, as only about 40% of the loaded drug was released (based on the in vitro release data) during the experimental period of 5 days. Since the medium and control nanoparticles without drug demonstrated similar growth curves, the antiproliferative effect seen with drug-loaded nanoparticles is because of the drug effect.

Confocal laser scanning microscopy demonstrated internalization of DOX-loaded nanoparticles in MCF-7 cells within 2 h of incubation (Figure 6c). Drug was seen localized in the cytoplasm, indicating that it is associated with nanoparticles. Similar experiments with drug in solution demonstrated nuclear localization of the drug. Since drug-loaded nanoparticles demonstrated cytotoxic effect, the drug may have been released slowly from the nanoparticles in the cytoplasm, and then diffused into the nucleus, the site of its action. Confocal microscopy of cells treated with drug-loaded nanoparticles for 24 and 48 h showed that the drug was localized in the nucleus. It is interesting to note that the fluorescence intensity in the nucleus was reduced slowly with incubation time in cells treated with drug in solution whereas it increased in cells treated with drug-loaded nanoparticles. Drug-loaded nanoparticles thus probably act as an intracellular depot and promote sustained drug retention.

Discussion

We have developed an innovative water-dispersible iron oxide nanoparticle-based formulation that can be loaded efficiently with water-insoluble anticancer agents. The drug-loaded formulations demonstrated sustained intracellular retention and dose-dependent antiproliferative activity in cancer cells. Magnetic nanoparticles generally are surface modified with hydrophilic polymers such as albumin,[21] dextran,[22−26] and starch[27] to disperse them in an aqueous vehicle; however, nanoparticles stabilized this way have limited application for drug delivery primarily because of the difficulty of loading these formulations with high doses of therapeutic agents, and especially with water-insoluble drugs. In a few studies, therapeutic agents are either conjugated chemically or bound through ionic interactions.[8−11] Alexiou et al.[6] studied magnetic particles coated with starch modified with phosphate groups, and the drug of interest, mitoxantrone, was ionically bound to the phosphate groups of the starch; however, the drug dissociated in about ∼60 min under in vitro conditions. Further, the amount of drug bound to the formulation is significantly lower (0.8 wt %) compared to that obtained with our formulation (8.2 wt %). High drug payload on a drug carrier system is necessary to achieve a therapeutic dose of the drug in the target tissue/organ more effectively. Rapid dissociation of drug from nanoparticles may result in its premature release in the blood stream, and hence the efficacy of the carrier system to target drug to the desired tissue/organ and retain it there for a sustained period of time could be significantly reduced.

In our formulation, hydrophobic drug partitions in the OA shell surrounding iron oxide nanoparticles, thus making the process much simpler than chemical conjugation methods used by others.[6,8−11] It also offers greater flexibility in terms of loading of different water-insoluble drugs either alone or in combination. Partitioning of DOX in OA was evident from the experiment in which a solution of DOX prepared in a 3:1 volume ratio of water to ethanol was shaken with an equal volume of OA. There was no change in the phase-volume ratio of OA to the water−ethanol phase, but most of the drug rapidly partitioned in the OA phase as apparent from the red color of the drug. We also have formulated paclitaxel-loaded nanoparticles using an identical procedure that demonstrated high efficiency of drug loading (data not shown). The drug-loading efficiency would probably depend on the partition coefficient of a particular drug between OA and the aqueous phase, and the amount of drug that can be dissolved in the OA shell associated with nanoparticles. We have not determined directly the effect of the amount of drug added and its encapsulating efficiency, but on the basis of the 82% encapsulation efficacy observed with DOX, it seems feasible to load large amounts of drug into the nanoparticles.

Our results demonstrated that OA is chemisorbed as a carboxylate headgroup on the surface of iron oxide nanoparticles. It thus is expected to provide better association of drug to nanoparticles with the surrounding OA shell acting as a drug reservoir. Similar chemisorption of OA has also been reported on cobalt nanoparticles synthesized in the presence of fatty acid.[28] The procedure of drug loading developed in this study for iron oxide nanoparticles thus should be viable for other magnetic nanomaterials. The loaded drug probably diffuses out from the OA shell under

(21) Renshaw, P. F.; Owen, C. S.; McLaughlin, A. C.; Frey, T. G.; Leigh, J. S., Jr. Ferromagnetic contrast agents: a new approach. *Magn. Reson. Med.* **1986**, *3*, 217−225.

(22) Hasegawa, M.; Hokkoku, S. Magnetic iron oxide-dextran complex and process for its production. U.S. Patent 4,101,435, 1978.

(23) Dutton, A. H.; Tokuyasu, K. T.; Singer, S. J. Iron-dextran antibody conjugates: General method for simultaneous staining of two components in high-resolution immunoelectron microscopy. *Proc. Natl. Acad. Sci. U.S.A.* **1979**, *76*, 3392−3396.

(24) Griffin, T.; Mosbach, K.; Mosbach, R. Magnetic biospecific affinity adsorbents for immunoglobulin and enzyme isolation. *Appl. Biochem. Biotechnol.* **1981**, *6*, 283.

(25) Molday, R. S.; MacKenzie, D. Immunospecific ferromagnetic iron-dextran reagents for the labeling and magnetic separation of cells. *J. Immunol. Methods* **1982**, *52*, 353−367.

(26) Schroder, U.; Mosbach, K. Intravascularly administrable, magnetically responsive nanosphere or nanoparticle, a process for the production thereof, and the use thereof. U.S. Patent 4,501,726, 1985.

(27) Veiga, V.; Ryan, D. H.; Sourty, E.; Llanes, F.; Marchessault, R. H. Formation and characterization of superparamagnetic crosslinked high-amylose starch. *Carbohydr. Polym.* **2000**, *42*, 353−357.

the influence of concentration gradient, but further investigation is required to understand the complete mechanism. The OA shell also can protect iron oxide nanoparticles from oxidation and/or hydrolysis in the presence of water, which can reduce significantly the magnetization of the formulation.[29]

Pluronics are block copolymers and are commonly used in micellar form as a drug carrier or for surface modification of colloidal drug carrier systems such as nanoparticles to prolong their systemic circulation time following intravenous administration.[30] Pluronics polymers have in their chains hydrophobic segments, polypropylene oxide (PPO) sandwiched between hydrophilic segments, polyethylene oxide (PEO).[31] We hypothesized that the hydrophobic segments of Pluronic anchor at the interface of the OA shell around iron oxide nanoparticles and the hydrophilic segments extend into the aqueous phase (Figure 1). Hydration of the PEO corona of Pluronic thus confers aqueous dispersity to the formulation as well as increases the hydrodynamic diameter of the iron oxide nanoparticles. Iron oxide nanoparticles without the OA shell could not be dispersed in Pluronic solution because it is not adsorbed onto the iron oxide nanoparticles as indicated by the FT-IR data (Figure 4c). This could be because of the hydrophilic nature of the surface of the iron oxide nanoparticles. The OA shell surrounding the iron oxide nanoparticles thus plays a dual role, i.e., as a drug reservoir and as an interface for anchoring the hydrophobic PPO chain of Pluronic to make the formulation water-dispersible.

One strategy for tumor targeting of anticancer agents using a colloidal carrier system is through the enhanced permeation retention (EPR) effect. Tumors have leaky vasculature and reduced lymphatic drainage, and hence intravenously injected colloidal systems extravasate and preferentially accumulate in the tumor tissue.[32] For magnetic nanoparticles to be successful for tumor targeting, they must evade the uptake by the reticuloendothelial system (RES) and remain in the blood circulation for a prolonged period of time. To avoid uptake by the RES, the surfaces of colloidal particles are modified with hydrophilic polymers (e.g., Pluronics, polyethylene glycol) to make them "stealth" from the RES. Pluronics with different ratios of PEO and PPO have been used to modify particle surfaces for this purpose.[30,33,34] We therefore anticipate that our iron oxide nanoparticle formulation, following modification with the appropriate Pluronic, can achieve a long blood circulation time, and thus could be effective in tumor targeting of anticancer agents via the EPR effect.

Systemic delivery of water-insoluble drugs is a challenge. Several drug delivery systems such as micelles, emulsions, and nanoparticle formulations have been investigated to address this problem. Commercially available Cremophor EL (BASF), which is a mixture of hydrogenated castor oils, is a commonly used formulation to dissolve hydrophobic drugs such as paclitaxel; however, it causes hypersensitivity reaction and does not provide adequate pharmacokinetics and drug distribution for effective tumor therapy.[35,36] Iron oxide nanoparticles are known to be well tolerated by the body and degrade with time.[37] Our formulation thus can be used as an effective drug delivery mechanism for systemic administration of a variety of hydrophobic agents.

Conclusions

The results of our studies demonstrated that OA-Pluronic-stabilized nanoparticles can be prepared and loaded effectively with hydrophobic drugs. The loaded drug is released slowly, and the drug-loaded nanoparticles demonstrated cellular uptake and cytotoxic effect of the encapsulated anticancer agent in a dose-dependent manner in cancer cell lines. The unique feature of our formulation is that it is theoretically possible to load any hydrophobic drug (or a combination of drugs) that can partition into the OA shell surrounding iron oxide nanoparticles. The formulation reported here thus can act as a universal drug carrier system for systemic administration of water-insoluble drugs. Although different formulations of iron oxide nanoparticles are being developed, this is the first report that has used the innovative approach of drug loading in the OA shell surrounding the magnetic core. Importantly, the formulation components and incorporated drug do not affect the magnetization properties of the core magnetic material. It is

(28) Wu, N.; Fu, L.; Su, M.; Aslam, M.; Wong, K. C.; Dravid, V. P. Interaction of Fatty Acid Monolayers with Cobalt Nanoparticles. *Nano Lett.* **2004**, *4*, 383−386.

(29) Hutten, A.; Sudfeld, D.; Ennen, I.; Reiss, G.; Hachmann, W.; Heinzmann, U.; Wojczykowski, K.; Jutzi, P.; Saikaly, W.; Thomas, G. New magnetic nanoparticles for biotechnology. *J. Biotechnol.* **2004**, *112*, 47−63.

(30) Moghimi, S. M.; Muir, I. S.; Illum, L.; Davis, S. S.; Kolb-Bachofen, V. Coating particles with a block co-polymer (poloxamine-908) suppresses opsonization but permits the activity of dysopsonins in the serum. *Biochim. Biophys. Acta* **1993**, *1179*, 157−165.

(31) Alexandridis, P.; Hatton, T. A. Poly(ethylene oxide)-poly(propylene oxide)-poly(ethylene oxide) block copolymer surfactants in aqueous solutions and at interfaces: thermodynamics, structure, dynamics, and modeling. *Colloid Surf., A* **1995**, *96*, 1−46.

(32) Maeda, H.; Seymour, L. W.; Miyamoto, Y. Conjugates of anticancer agents and polymers: advantages of macromolecular therapeutics in vivo. *Bioconjugate Chem.* **1992**, *3*, 351−362.

(33) Moghimi, S. M.; Hedeman, H.; Christy, N. M.; Illum, L.; Davis, S. S. Enhanced hepatic clearance of intravenously administered sterically stabilized microspheres in zymosan-stimulated rats. *J. Leukocyte Biol.* **1993**, *54*, 513−517.

(34) Kong, G.; Braun, R. D.; Dewhirst, M. W. Characterization of the effect of hyperthermia on nanoparticle extravasation from tumor vasculature. *Cancer Res.* **2001**, *61*, 3027−3032.

(35) Weiss, R. B.; Donehower, R. C.; Wiernik, P. H.; Ohnuma, T.; Gralla, R. J.; Trump, D. L.; Baker, J. R., Jr.; Van Echo, D. A.; Von Hoff, D. D.; Leyland-Jones, B. Hypersensitivity reactions from taxol. *J. Clin. Oncol.* **1990**, *8*, 1263−1268.

(36) Gelderblom, H.; Verweij, J.; van Zomeren, D. M.; Buijs, D.; Ouwens, L.; Nooter, K.; Stoter, G.; Sparreboom, A. Influence of Cremophor El on the bioavailability of intraperitoneal paclitaxel. *Clin. Cancer Res.* **2002**, *8*, 1237−1241.

(37) Okon, E.; Pouliquen, D.; Okon, P.; Kovaleva, Z. V.; Stepanova, T. P.; Lavit, S. G.; Kudryavtsev, B. N.; Jallet, P. Biodegradation of magnetite dextran nanoparticles in the rat. A histologic and biophysical study. *Lab. Invest.* **1994**, *71*, 895−903.

possible to functionalize our nanoparticles with ligands or antibodies to further enhance their therapeutic potential, including as agents for magnetic imaging.

Acknowledgment. This work is supported by a grant from the Nebraska Research Initiative.
MP0500014